Near-Infrared Emitting Poly(amidoamine) Dendrimers with an Anthraquinone Core toward Versatile Non-Invasive Biological Imaging

Kamal Jouad, Svetlana Eliseeva, Guillaume Collet, Cyril Colas, David da Silva, Marie-Aude Hiebel, Nabil El Brahmi, Mohamed Akssira, Stephane Petoud, Saïd El Kazzouli, et al.

Near-infrared Emitting Poly(amidoamine) Dendrimers with an Anthraquinone Core towards Versatile Non-invasive Biological Imaging

Kamal Jouad[$,#], Svetlana V. Eliseeva[£], Guillaume Collet[£,+], Cyril Colas[$,£] David Da Silva[$], Marie-Aude Hiebel[$], Nabil El Brahmi[#], Mohamed Akssira[&], Stéphane Petoud[£,*], Saïd El Kazzouli[#,*] and Franck Suzenet[$,*]

[$] Institut de Chimie Organique et Analytique UMR 7311, Université d'Orléans Rue de Chartres BP 6759 45067. Orléans Cedex 2 France.

[#] Euromed Research Center, Euromed Faculty of Pharmacy, Euromed University of Fes, Route de Meknes, 30000 Fez, Morocco.

[£] Centre de Biophysique Moléculaire, CNRS UPR 4301, Rue Charles Sadron, 45071 Orléans Cedex 2 France.

[&] Faculty of Sciences and Technologies of Mohammedia, URAC 22 FSTM, University Hassan II, BP 146, 28800 Mohammedia, Morocco.

[+] Le Studium Loire Valley Institute for Advanced Studies, Orléans & Tours, France

KEYWORDS: anthraquinone, poly(amidoamine) (PAMAM) dendrimer, near-infrared, chromophore, water-soluble probe, optical biological imaging, non-invasive.

ABSTRACT: Today, there is a very strong demand for versatile near-infrared imaging (NIR) agents suitable for non-invasive optical imaging in living organisms (in vivo imaging). We created here a family of NIR emitting macromolecules that take advantage of the unique structure of dendrimers. In contrast to existing fluorescent dendrimers bearing fluorophores at their periphery or in their cavities, a NIR fluorescent structure is incorporated in the core of the dendrimer. By using the poly(amidoamine) dendrimer structure, we want to promote the biocompatibility of the NIR-emissive system and to have functional groups available at the periphery to obtain specific biological functionalities such as the ability to deliver drugs or for targeting biological location. We report here the divergent synthesis and characterization by NMR and mass spectrometries of poly(amidoamine) dendrimers derived from the fluorescent NIR-emitting anthraquinone core (**AQ-PAMAF**). **AQ-PAMAFs** ranging from the generation -0.5 up to 3 were synthesized with a good level of control resulting in homogeneous and complete dendrimers. Absorption, excitation and emission spectra as well as quantum yields of **AQ-PAMAF** have been determined in aqueous solutions and compared with the corresponding properties of the **AQ**-core. It has been demonstrated that absorption bands of **AQ-PAMAF** range from UV to 750 nm while the emission is observed in the range of 650 to 950 nm. Fluorescence macroscopy experiments confirmed that the NIR signal of **AQ-PAMAF** can be detected with a satisfactory signal-to-noise ratio in aqueous solution, in blood and through 1 mm thick tissue-mimicking phantom. Results show that our approach is highly promising for the creation of an unprecedented generation of versatile NIR-emitting agents.

Introduction

The use of near-infrared (NIR) light is triggering a growing interest in the last two decades for in vitro and in vivo applications. In this range of wavelength (> 650 nm), also called the biological imaging window,[1] native biomolecules exhibit low absorption and autofluorescence resulting in a significant reduction of the background signal. A relatively deep penetration of light through tissues (>1 cm depth) can be obtained and thanks to the low interaction between light and biological material, risks of disturbing or damaging the biological systems and/or their metabolism is minimized.[2–6] In addition, optical imaging based on fluorescence allow to reach a high detection sensitivity by using rather inexpensive and transportable equipment.[7] Images acquired in the NIR range possess higher resolution compared to those measured in the visible due to the lower scattering of light in this wavelength

For an optimal benefit in NIR optical bioimaging, probes have i) to be excited at low energy and emit in the NIR, ii) to be soluble in biological media, iii) to be photostable and, ideally, iv) to be able to carry and to monitor the delivery of molecules such as drugs. So far, such probes remain limited to few systems of different chemical natures (1) organic dyes, (2) fluorescent organic/inorganic nanostructures,[8] and (3) quantum dots (QDs).[6]

In the last decade, the fluorescent probe domain has been extended to dendrimer one.[9,10,11,12,13,14] Due to their particular architectures, dendrimers and especially fluorescent dendrimers have been used in many fields of science, with a special emphasis on biology, to monitor and understand biological events at the molecular level.[15,16,17] As an example, Majoral and Caminade have recently reviewed the family of phosphorhydrazone dendrimers containing fluorescent groups in different parts of the dendritic structure (core, branch and surface).[18] The fluorescent properties were very often controlled by the dendrimer structure and one visible phthalocyanine chromophore was incorporated as the core of the dendrimer structure.[19] In contrast, poly(amidoamine) dendrimers, extensively used for different types of applications, were less often designed to generate fluorescence properties.[20] To reach this goal, two strategies have been explored either by incorporating fluorescent entities in the internal cavity of the dendrimer tree[21] or by grafting the fluorescent entities in the end of the branches of the dendrimer. This last approach has been so far the most successful way to generate poly(amidoamine) dendrimers with promising fluorescent properties.[22,23]

Taking into account these previous works and considering the work of Tomalia showing that the poly(amidoamine) dendrimer have demonstrated a good biocompatibility,[24,25] but also a high water solubility to the point that they can be used as water-solubility enhancer,[20,26,27] we have decided to design, synthesize and characterize a new type of fluorescent poly(amidoamine) dendrimers in which the chromophore is located in the core of the dendrimers structure. With this strategy, the dendrimer will maintain its aqueous solubility and available functionalities at the periphery (amine or carboxylic acid functions). This fluorescent macromolecule will offer large opportunities to link biomolecules and/or drugs to target and/or deliver drugs respectively and to decrease the poly(amidoamine) toxicity. Very few works on the bases of this concept have been published. The first reported example is the synthesis of G2.5 fluorescent labeled poly(amidoamine) dendrimers possessing a naphthalene core.[28] Later, low generation (Go, 4 amino-terminated groups) poly(amidoamine) dendrimer built around perylene diimide chromophore were tested as sensor with selectivity toward metal ion in organic solvent.[29] More recently, the same hydrophobic fluorophore was conjugated with hydrophilic poly(amidoamine) dendrons to obtain a series of fluorescent dendrimers with enhanced water-solubility for fluorescence imaging in biological conditions.[18] Another example has been reported by Christensen, J. B et al., with the synthesis of a dendrimer with a single sulforhodamine B molecule as the core.[30,31] Several works were also devoted to the development of fluorescent macromolecules with poly(amidoamine) dendrons functionalized with chromophores localized at the focal point and/or at the periphery of the dendron.[32–35] It is important to note here that none of these works were targeted the development of NIR absorbing and emitting poly(amidoamine) dendrimers.

In this present work, we report the design, synthesis and characterization of a novel class of anthraquinone-functionalized poly(amidoamine) dendrimers (**AQ-PAMAFs**) up to the third generation as a new NIR optical imaging probe. The synthetic pathway allows to obtain a perfect characterization of each dendrimer generation by 1H NMR that confirm a high degree of purity. The characterization of both NIR luminescence and biological properties of this macromolecules are described. Anthraquinone **11** was selected for its low energy absorption thanks to the methoxy and amino electron-donating groups on the scaffold [36–43] and consequently was chosen as a core candidate because of its light absorption capability in the biological window as well as its symmetric structure which is desirable to ease the synthesis.

RESULTS AND DISCUSSION

Chemical synthesis and characterization

The anthraquinone-core poly(amidoamine) dendrimers (**AQ-PAMAFs**) were prepared by a divergent synthesis inspired by a previously described repetitive sequence[30,44] starting from the anthraquinone-core **11** and followed by a Michael addition on methyl acrylate and an amidation reaction with the help of ethylenediamine. In order to maintain a planar symmetry, and thus to simplify the characterization of the different dendrimer generations, we decided to start with two ethylamino arms at positions 1 and 4 of the anthraquinone core. For this purpose, the key intermediate **8** was synthesized in seven steps according to literature procedures[45] (Scheme 1). Then, the fluoro groups were substituted with Boc-ethylenediamine in the presence of pyridine at 100 °C for 32 h giving the desired di-substituted product **10** (**AQ-core**) in 85% yield. The hydrolysis of the Boc protecting groups was performed in a mixture of trifluoracetic acid (TFA)/dichloromethane under an optimized 0 °C temperature condition (to avoid side product formation, see SI) for 1.5 h yielding to the TFA salt **11** as a unique product.

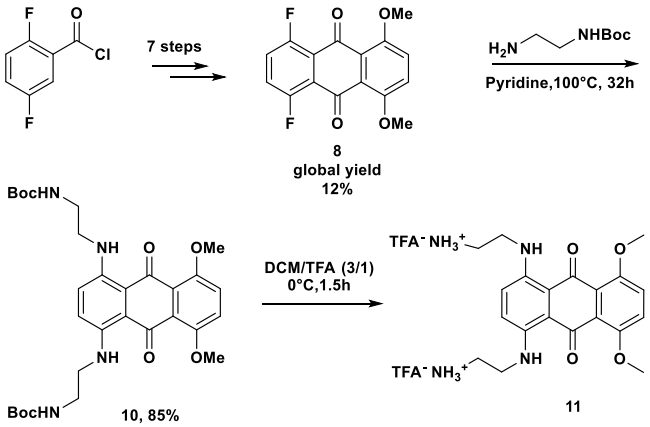

Scheme 1. Synthetic pathway of the anthraquinone core 11

The deprotected diaminoanthraquinone salt **11** was then engaged in a Michael addition with an excess of methyl acrylate in the presence of triethylamine at 45 °C for 3 days to offer the desired product **G-0.5** in 71% yield (Scheme 2),

referred to as a half-generation of the anthraquinone-poly(amidoamine) dendrimer (**AQ-PAMAF G-0.5**). The next condensation step performed under inert nitrogen atmosphere in MeOH with an excess of ethylenediamine for 5 days yielded the desired generation zero of the poly(amidoamine) shells **AQ-PAMAF Go** in 98% yield.

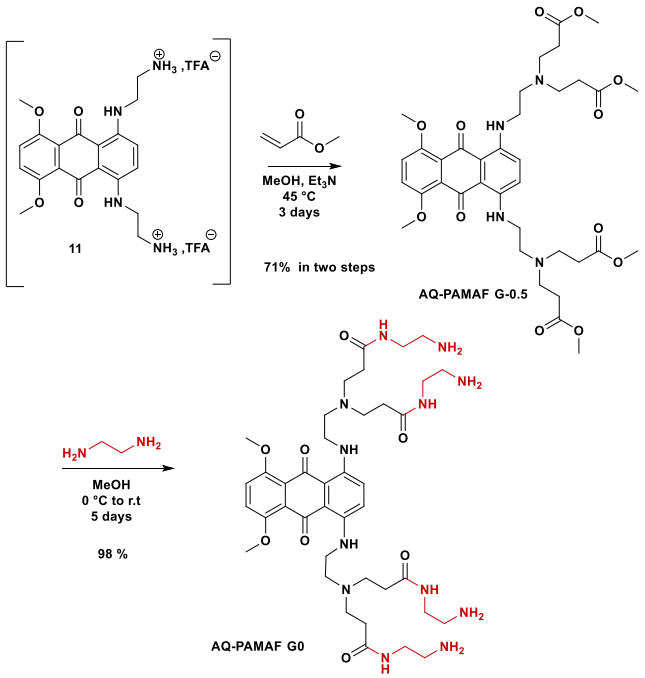

Scheme 2. Synthetic pathway of AQ-PAMAF Go

At this stage, a two-step iterative process (Michael addition with methyl acrylate and amidation with ethylendiamine) was engaged for the synthesis of higher-generations of **AQ-PAMAF** dendrimers (Scheme 3). These sequences yielded to various **AQ-PAMAF** dendrimers with 8 (**AQ-PAMAF G1**) and 16 (**AQ-PAMAF G2**) amine end of the branches groups in 98 and 97 % yield, respectively, after purification by size-exclusion chromatography. For the **AQ-PAMAF G3** with 32 amine end groups, the reaction was more sensitive than for the lower generations and let to products with a lower level of purity as often reported for high dendrimer generations. After careful optimization of the reaction conditions (solvent free conditions) and purification, the **G3** dendrimer was isolated in 9 days from the **AQ-PAMAF G2.5** with a 23% overall yield from **10** (**AQ-core**).

It is important to notice that each **AQ-PAMAF** dendrimer generation was fully characterized by NMR (^{1}H and ^{13}C) and mass spectrometry (MALDI-TOF MS and ESI-QTOF HRMS) analysis and their purities were evaluated by ^{1}H NMR. Thanks to the high level of symmetry in the **AQ-PAMAF** dendrimer structures, all the terminal groups are chemically equivalent and the NMR signals for the dendrimer core are therefore highly reduced despite the size of the macromolecule, allowing a rapid and easy analysis of the ^{1}H NMR data. As an illustration (Figure 1), spectra of **AQ-PAMAF G-0.5** to **G3** are stacked and clearly show the poly(amidoamine) arms incorporation characterized by signals at 2.3-3.6 ppm and the presence of the **AQ** dendritic core unambiguously characterized by signals at *ca.* 7.10-7.25 and 3.9 ppm. Any loss in symmetry which would be due to incomplete Michael addition, intramolecular cyclisation, or retro-Michael addition, would result in additional signals in the ^{1}H NMR spectrum. Furthermore, the dendrimer grew from a half generation (**AQ-PAMAF G-0.5**, **Go.5**, **G1.5**, **G2.5**) to the following full generation (**AQ-PAMAF Go, G1, G2, G3**

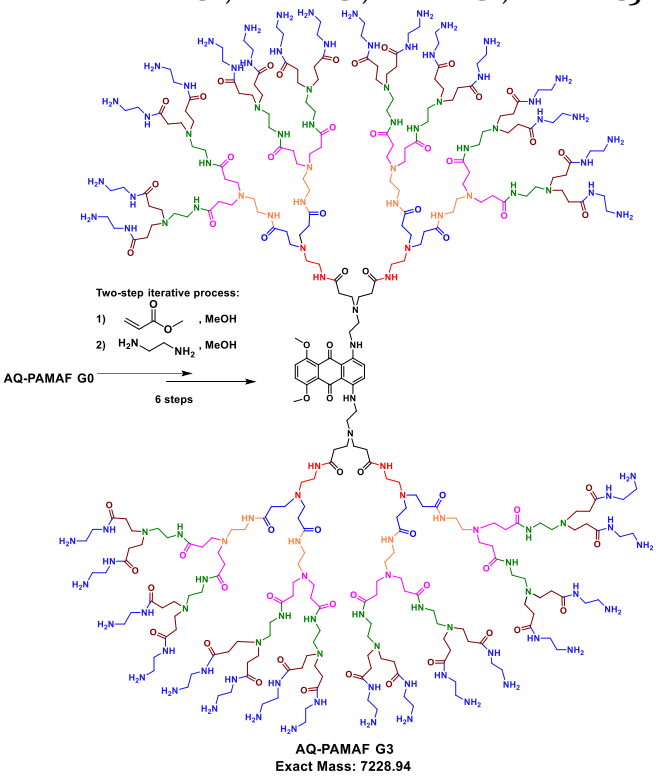

Scheme 3. Scheme depicting the divergent growth of AQ-PAMAF G3

respectively) was efficiently and easily monitored by the appearance/disappearance of the methyl esters signal on the surface of the dendrimer at 3.66 ppm. These observations were corroborated by the ^{13}C NMR spectrum analysis, which allows an easy and efficient control of the dendrimer growth thanks to the appearance of the new carbon signals while the anthraquinone carbons shifts are unchanged (see SI, Figure S2). The characterization of each generation and half generation was also clearly established by MALDI-TOF and HRMS (see SI, Figures S3 and S4). Thanks to this fine MALDI-TOF analysis (see SI, Figure S6), we have found that a side dendrimer **AQ-PAMAF G'1.5** with structural defects was produced from the divergent incomplete growth caused by two retro-Michael and intramolecular cyclization reactions (See SI, Scheme S5). This structural defect was also observed by ^{1}H NMR which showed that the anthraquinone (**AQ**) ring-based dendrimer lose its symmetry by showing two doublet signals instead of two singlets of aromatic protons (see SI, Figure S7).

To overcome this growth defects caused by unwanted intramolecular cyclization and to obtain the desired **AQ-PAMAF G2** which is completely decorated on the surface, we decided to use *N*-Boc-ethylenediamine for the amidation step. The optimization of this reaction conditions

allowed us to isolate the **AQ-PAMAF-Boc G2** with a good purity (as determined by ^{1}H NMR) and in 86% yield by using an excess of *N*-Boc-ethylenediamine at 45 °C for 40 days (Scheme 5). The longer reaction time may be due to the restricted access to the ester groups hindered by the bulky N-Boc protecting groups.

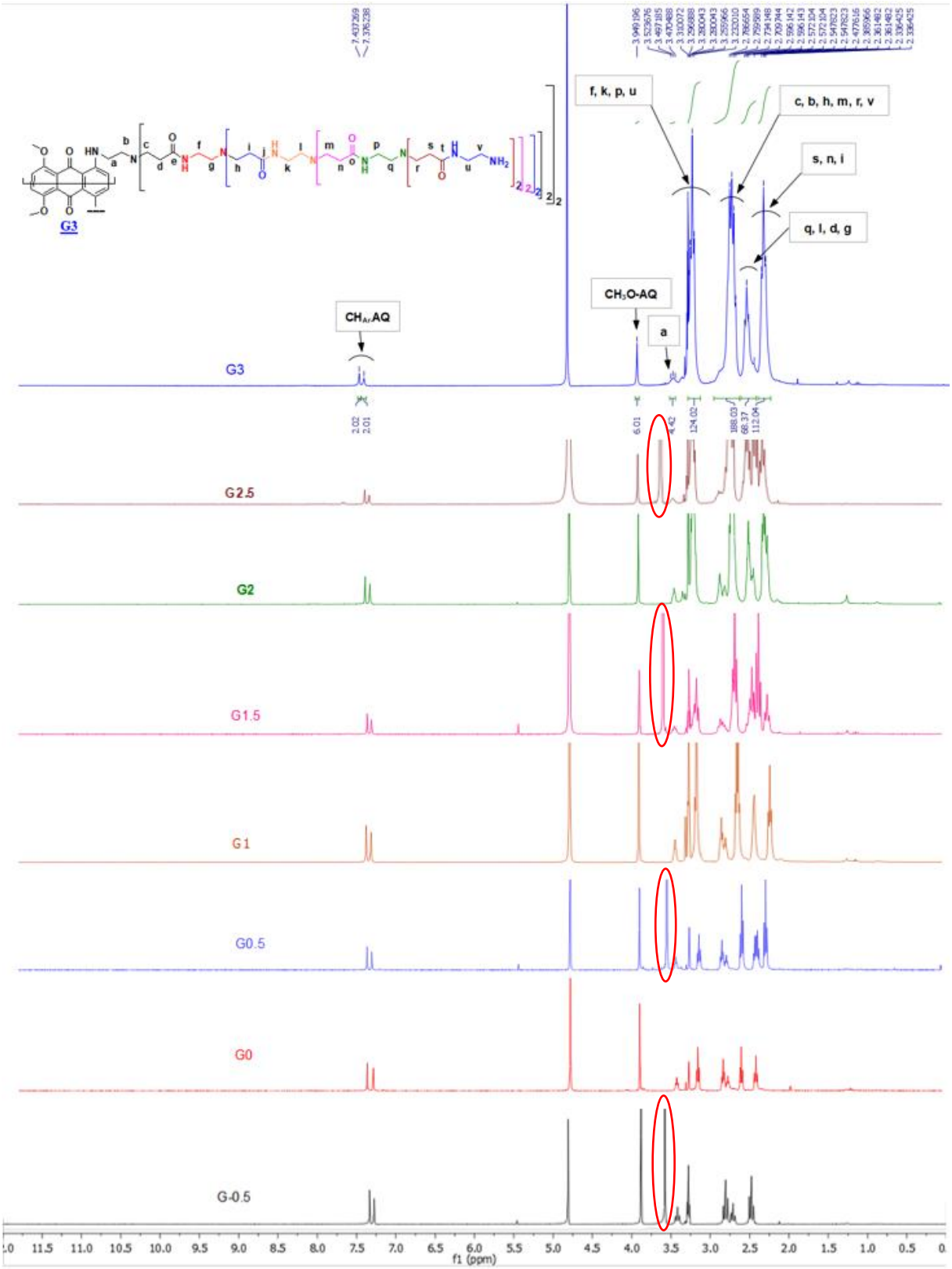

Figure 1. ^{1}H NMR spectra of dendritic growth

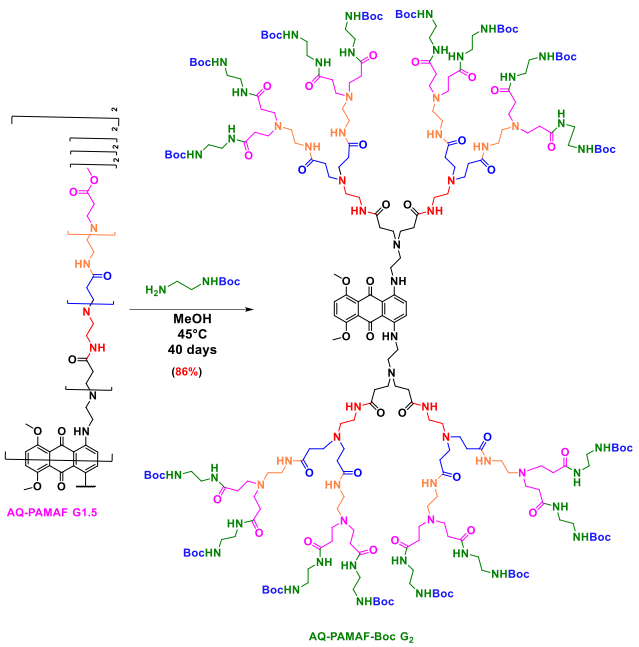

Scheme 5. Schematic pathway of the synthesis of AQ-PAMAF-Boc G2

This synthetic step was monitored by ^{1}H NMR and the spectrum showed a chemical shift of the Boc groups at 1.43 ppm (144 H) which clearly indicated the successful amidation reaction (see SI, Dendrimer **AQ-PAMAF-Boc G2** description and spectra). In addition, HRMS spectrum confirm the mass of the expected product $[M+4H]^{4+}$=1295.8154 with a good isotopic pattern in agreement with the theoretical calculation (see SI, Dendrimer **AQ-PAMAF-Boc G2** description). Despite the high level of control of the structure and of the resulting purity of the **AQ-PAMAF-Boc G2**, first attempts to deprotect the NH-Boc groups were unsuccessful. As a consequence, generations 2, 2.5 and 3 were finally synthesized thanks to the initial two-step iterative process. The optimization of the reaction conditions by increasing the excess of ethylene diamine (up to free solvent conditions for the synthesis of generation 3), **AQ-PAMAF G2**, **AQ-PAMAF G2.5** and **AQ-PAMAF G3** were purified and isolated by size-exclusion chromatography and were fully characterized (vide supra).

Characterization of the Photophysical Properties

The photophysical properties of the different generations of the hydrophilic **AQ-PAMAF** dendrimers (**Go.5** to **G3**) were evaluated in aqueous solutions while those of the core (**AQ-core, 10**) were measured in DMSO because of the limited solubility of the anthraquinone (Figure **2,** Table 1). Absorption spectra of the **AQ-core** and the **AQ-PAMAF** dendrimers exhibit similar broad absorption bands from the UV to the visible and in the NIR range up to 750 nm (Figure **2**, black traces) which can be attributed to $\pi\rightarrow\pi^*$ and to $n\rightarrow\pi^*$ transitions.[42,46] Two pronounced low-energy maxima can be observed. For the solutions of **AQ-PAMAF** dendrimers in water, the positions of the maxima vary slightly, *i.e.* from 617.5 to 624.5 nm and from 664.5 to 675 nm, depending on the nature and the number of the terminal groups. A small bathochromic shift observed for the different generations of the **AQ-PAMAF** dendrimers compared to the hydrophobic **AQ-core** can be induced by a solvent effect or by the growth of the poly(amidoamine) branches.[47] Under excitation into the absorption bands at 625 nm all studied compounds show broad-band emission in the range of 650-950 nm (Figure 2, red traces). Emission spectra of aqueous solutions of G0.5, G1.5 and G2.5 possessing methyl ester groups at their periphery are almost identical. General envelopes of the emission spectra of aqueous solutions of G1, G2 and G3 display slight variations but no specific dependence with the generation could be identified. Such changes might be caused by the environmental modulation of the fluorescent **AQ-core** with the growth of the dendrimer branches and their different folding. Excitation spectra collected upon monitoring the emission at 750 nm (Figure 2, blue traces) show that the shapes of these bands resemble the one observed on the absorption spectra (Figure 2, black traces).

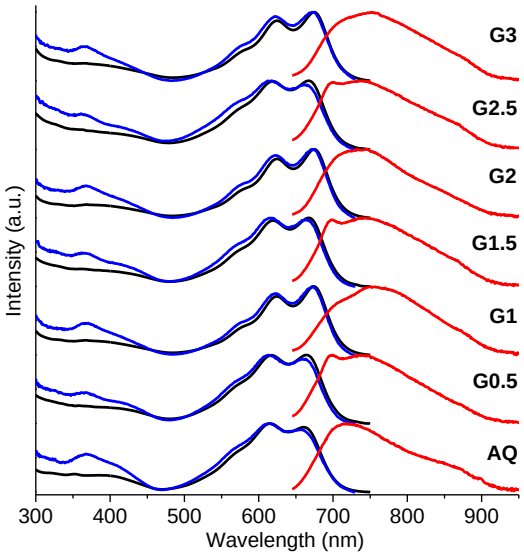

Figure 2. Normalized absorption (black traces), excitation (blue traces, λ_{em} = 750 nm) and emission (red traces, λ_{ex} = 625 nm) spectra recorded for the solutions of the **AQ-core** (20 µM, DMSO) and for the corresponding generations of the **AQ-PAMAF** dendrimers (**Go.5** to **G3**; 20 µM, H_2O) at room temperature.

The values of the absolute quantum yields of the NIR emission were determined and lie in a narrow range of 0.11-0.19% (Table 1). These results indicate that the electronic structure of the anthraquinone chromophore is minimally affected by the growth of poly(amidoamine) branches, as well as by the nature and the number of the terminal

groups. Altogether, the photophysical properties of the different generations of hydrophilic **AQ-PAMAF** dendrimers, *i.e.* the excitation in the red-NIR range and the emission in the NIR domain with a satisfactory brightness, suggest these macromolecules to be promising candidates for NIR optical imaging studies.

Table 1. Photophysical properties recorded for the solutions of the AQ-core (20 µM, DMSO) and the corresponding generations of the AQ-PAMAF dendrimers (G0.5 to G3; 20 µM, H_2O) at room temperature.

Compound	Nature and number of the terminal groups	λ_{abs} (nm)[a]	ε (M^{-1} cm^{-1})[a]	Φ (%)[b]
AQ-core	AQ-$(CH_2$-CH_2-NHBoc$)_2$	615.5; 660.5	14240 ; 13475	0.189(1)
G0.5	AQ-PAMAF-$(CO_2CH_3)_8$	617.5; 664.5	12302 ; 12360	0.151(1)
G1	AQ-PAMAF-$(NH_2)_8$	624.0; 674.0	13238 ; 15443	0.176(1)
G1.5	AQ-PAMAF-$(CO_2CH_3)_{16}$	619.0; 667.0	12408 ; 12909	0.146(1)
G2	AQ-PAMAF-$(NH_2)_{16}$	624.5; 675.0	13267 ; 15391	0.114(1)
G2.5	AQ-PAMAF-$(CO_2CH_3)_{32}$	619.0; 667.0	13744 ; 15511	0.164(1)
G3	AQ-PAMAF-$(NH_2)_{32}$	624.5; 675.0	13652 ; 15535	0.158(1)

[a] From absorption spectra (Figure 2, S8); maxima in the range 470-750 nm. [b] Absolute quantum yield upon 625 nm excitation; 2σ values are given between parentheses.

NIR fluorescence imaging

Considering the ability of **AQ-PAMAF** dendrimers to absorb and to emit photons at wavelengths compatible with experiments in biological conditions that have been revealed by spectroscopy, NIR fluorescence optical imaging was carried out to demonstrate their ability to operate in real experimental conditions. To achieve this goal, we designed experiments simulating an ultimate *in vivo* imaging experiment conducted on mice.

Stock solutions of **AQ-PAMAF** dendrimers were diluted in both (i) water and (ii) blood to 200 µM concentration, and then introduced into small capillaries in order to mimic blood vessels upon a systemic injection of compounds (Figure 3). Epifluorescence macroscopy imaging experiments conducted with these capillaries indicated that upon excitation with light passing through a 650 nm band pass 50 nm filter **AQ-PAMAF** dendrimers maintain their abilities to emit a bright signal in the NIR when diluted either in water (Figure 3A) or in blood (Figure 3B). The fact that an impressive intensity of NIR emission of **AQ-PAMAF** dendrimers was observable in blood (Figure 3B) should be particularly highlighted. The strong absorption and scattering of light and autofluorescence of blood create a very difficult challenge for the recording of good quality images through this medium. Interestingly, despite the great similarity of the values of luminescence quantum yields recorded for the different generations of **AQ-PAMAF** dendrimers (Table 1) in pure water, an enhanced NIR signal intensity was observed for the dendrimers of higher generations, in particular for the **G2.5** and **G3**. In addition, the collected NIR images indicated the absence of any aggregation of **AQ-PAMAFs** at the used optical resolution opening possibilities for *in vivo* imaging applications upon intravenous injections. These observations promote the interest of the advanced chemistry used in this work to enhance further the biocompatibility and the optical properties of **AQ** derivatives. Through the growth of poly(amidoamine) branches of these dendrimers, the **AQ** fluorophore maintains its fluorescent properties while being water soluble.

In view of the strong signal of the NIR emission observed for the higher generations of **AQ-PAMAF** dendrimers, further imaging experiments were performed through a depth of 1 mm of bio-mimicking phantom tissue placed on the top of capillaries filled with blood containing **AQ-PAMAF G2.5** and **G3** dendrimers.[48] For both **G2.5** and **G3** dendrimers (Figures 3C and 3D), a NIR signal was detected with a sufficient signal-to-noise ratio resulting in the acquisition of good quality image of the blood-filled capillaries containing **AQ-PAMAF** dendrimers through the phantom tissue. Finally, high quality images obtained with **AQ-PAMAF G2.5** and **G3** through 1 mm of bio-mimicking tissue highlight the great potential of the higher generations of dendrimers for *in vivo* applications.

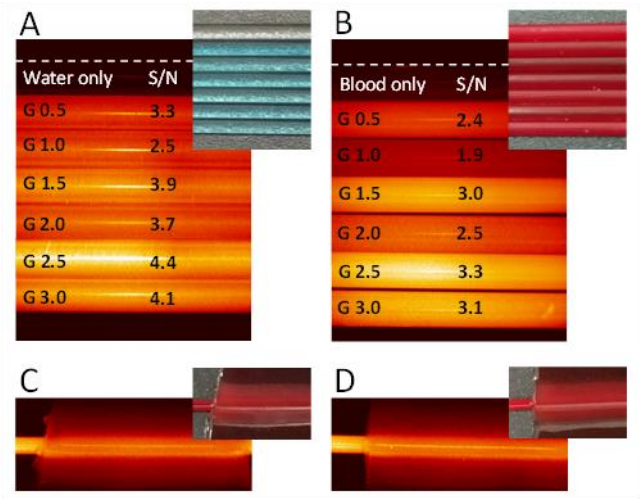

Figure 3. NIR fluorescence macroscopy images of capillaries filled with **AQ-PAMAF** dendrimers of different generations diluted at 200 µM in water (A) or in mouse blood (B). From top to bottom, the series of capillaries contain water/blood exclusively as a control, and then **AQ-PAMAF** dendrimers of generations **G0.5**, **G1**, **G1.5**, **G2**, **G2.5**, and **G3** respectively. The fluorescence signals arising from capillaries containing **AQ-PAMAF G2.5** (C) and **AQ-PAMAF G3** (D) at 200 µM in mouse blood were recorded through a 1 mm thick bio mimicking

phantom tissue. Epifluorescence pictures were obtained using the following filters and exposure times: λ_{ex} = 650 nm band pass 50 nm, λ_{em} = 716 nm band pass 40 nm, τ_{exp} = 5 s for A and B, τ_{exp} = 10 s for C and D. The orange color was chosen to artificially represent the NIR fluorescence arising from the dendrimers. Top right corner images correspond to color pictures of the samples to show the experimental setup.

CONCLUSION

In conclusion, we have successfully designed and synthesized a third generation **AQ-PAMAF**-dendrimer with an efficient synthetic route that includes 17 steps with a 3% global yield. Each generation of dendrimer was unambiguously isolated and characterized by ^{1}H NMR and mass spectrometry. We have shown the high efficiency of ^{1}H NMR spectroscopy for the monitoring and characterization of poly(amidoamine) dendrimers growth from low to high generation. Hydrophilic poly(amidoamine) dendrimer tree were built around a near infrared emitting chromophore located in the core of the dendrimer structure. The photophysical properties of the different generations of **AQ-PAMAF** dendrimers, i.e. excitation in the red-NIR range and emission in the NIR domain with good brightness combined with the high-quality of the NIR macroscopy images of dendrimers solution in water and blood obtained with **AQ-PAMAF G2.5** and **G3** through bio-mimicking tissue highlight the great potential of the higher generations of dendrimers for in vivo NIR imaging applications. Such hydrophilic and biocompatible dendrimer NIR imaging probe open new routes for the design of new nano-object that could combine the role of nanocarrier of drugs and/or vectors while being a NIR imaging agents due to their branches that are available to allow for a versatile functionalization.

ACKNOWLEDGMENT

Thanks are due to the Campus France (PHC-Toubkal 2017 (French-Morocco bilateral program Grant Number: 36875XJ), Euromed University of Fes and The University of Orleans for financial support as well as the Ligue contre le Cancer. Authors also gratefully acknowledge the projects CHemBio (FEDER-FSE 2014-2020-EX003677), Techsab (FEDER-FSE 2014-2020-EX011313), the RTR Motivhealth (2019-00131403) and the Labex programs SYNORG (ANR-11-LABX-0029) and IRON (ANR-11-LABX-0018-01) for their financial support of ICOA, UMR 7311, University of Orléans, CNRS. S.P. acknowledges support from Institut National de la Santé et de la Recherche Médicale (INSERM). Mouse blood was kindly provided by Mr Rudy Clemençon.

ASSOCIATED CONTENT

Supporting Information.
Full experimental details and spectral data for products **9**, **10** and all dendrimer generations. This material is available free of charge via the Internet at http://pubs.acs.org.

AUTHOR INFORMATION

Corresponding Authors

Franck Suzenet - Institut de Chimie Organique et Analytique, UMR 7311, Université d'Orléans, Rue de Chartres, BP 6759 45067 Orléans Cedex 2 France;
orcid.org/ 0000-0003-1394-1603;
Email : franck.suzenet@univ-orleans.fr
Said El Kazzouli - Euromed Research Center, Euromed Faculty of Pharmacy, Euromed University of Fes, Route de Meknes, 30000 Fez, Morocco;
orcid.org/0000-0001-5021-3571;
Email : s.elkazzouli@ueuromed.org
Stéphane Petoud - Centre de Biophysique Moléculaire, CNRS UPR 4301, Rue Charles Sadron, 45071 Orléans Cedex 2 France ;
orcid.org/0000-0003-4659-4505;
Email : stephane.petoud@inserm.fr

Authors

Kamal Jouad - Institut de Chimie Organique et Analytique, UMR 7311, Uni-versité d'Orléans, Rue de Chartres, BP 6759 45067 Orléans Cedex 2 France; Euromed Research Center, Euromed Faculty of Pharmacy, Euromed University of Fes, Route de Meknes, 30000 Fez, Morocco;
Svetlana V. Eliseeva - Centre de Biophysique Moléculaire, CNRS UPR 4301, Rue Charles Sadron, 45071 Orléans Cedex 2 France ;
orcid.org/0000-0002-1768-8513
Guillaume Collet - Centre de Biophysique Moléculaire, CNRS UPR 4301, Rue Charles Sadron, 45071 Orléans Cedex 2 France ;
orcid.org/0000-0002-0355-563X
Cyril Colas - Institut de Chimie Organique et Analytique UMR 7311, Université d'Orléans Rue de Chartres BP 6759 45067. Orlé-ans Cedex 2 France; Centre de Biophysique Moléculaire, CNRS UPR 4301, Rue Charles Sadron, 45071 Orléans Cedex 2 France ;
orcid.org/0000-0003-1651-6813
David Da Silva - Institut de Chimie Organique et Analytique UMR 7311, Université d'Orléans Rue de Chartres BP 6759 45067. Orléans Cedex 2 France;
orcid.org/0000-0002-8760-6018.
Marie-Aude Hiebel - Institut de Chimie Organique et Analytique UMR 7311, Université d'Orléans Rue de Chartres BP 6759 45067. Orléans Cedex 2 France;
orcid.org/ 0000-0001-9476-9176.
Nabil El Brahim - Euromed Research Center, Euromed Faculty of Pharmacy, Euromed University of Fes, Route de Meknes, 30000 Fez, Morocco;
Mohamed Akssira - Faculty of Sciences and Technologies of Mohammedia, URAC 22 FSTM, University Hassan II, BP 146, 28800 Mo-hammedia, Morocco
orcid.org/ 0000-0001-8867-2837;

Author Contributions

The manuscript was written through contributions of all authors.

ACKNOWLEDGMENT

Thanks are due to the CAMPUS FRANCE (PHC-TOUBKAL 2017 (French-Morocco bilateral program Grant Number: 36875XJ), Euromed University of Fes and The University of Orleans for financial support as well as the Ligue contre le Cancer. Authors also gratefully acknowledge the projects CHemBio (FEDER-FSE 2014-2020-EX003677), Techsab

(FEDER-FSE 2014-2020-EX011313), the RTR Motivhealth (2019-00131403) and the Labex programs SYNORG (ANR-11-LABX-0029) and IRON (ANR-11-LABX-0018-01) for their financial support of ICOA, UMR 7311, University of Orléans, CNRS. S.P. acknowledges support from Institut National de la Santé et de la Recherche Médicale (INSERM). Mouse blood was kindly provided by Mr Rudy Clemençon.

REFERENCES

(1) Pansare, V. J.; Hejazi, S.; Faenza, W. J.; Prud'Homme, R. K. Review of Long-Wavelength Optical and NIR Imaging Materials: Contrast Agents, Fluorophores, and Multifunctional Nano Carriers. *Chem. Mater.* **2012**, *24* (5), 812–827.

(2) Weissleder, R. A Clearer Vision for in Vivo Imaging: Progress Continues in the Development of Smaller, More Penetrable Probes for Biological Imaging. *Nat. Biotechnol.* **2001**, *19* (4), 316–317.

(3) Frangioni, J. V. In Vivo Near-Infrared Fluorescence Imaging. *Curr. Opin. Chem. Biol.* **2003**, *7* (5), 626–634.

(4) Umezawa, K.; Nakamura, Y.; Makino, H.; Citterio, D.; Suzuki, K. Bright, Color-Tunable Fluorescent Dyes in the Visible-near-Infrared Region. *J. Am. Chem. Soc.* **2008**, *130* (5), 1550–1551.

(5) Hemmer, E.; Benayas, A.; Légaré, F.; Vetrone, F. Fluorescent Aliphatic Hyperbranched Polyether: Chromophores-Free and without Any N and P Atoms. *Nanoscale Horiz.* **2015**, *00* (1–3), 1–22.

(6) Martinić, I.; Eliseeva, S. V.; Petoud, S. Near-Infrared Emitting Probes for Biological Imaging: Organic Fluorophores, Quantum Dots, Fluorescent Proteins, Lanthanide(III) Complexes and Nanomaterials. *J. Lumin.* **2017**, *189*, 19–43.

(7) Cieslikiewicz-Bouet, M.; Eliseeva, S. V.; Aucagne, V.; Delmas, A. F.; Gillaizeau, I.; Petoud, S. Near-Infrared Emitting Lanthanide(Iii) Complexes as Prototypes of Optical Imaging Agents with Peptide Targeting Ability: A Methodological Approach. *RSC Adv.* **2019**, *9* (3), 1747–1751.

(8) Cong, H.; Wang, K.; Zhou, Z.; Yang, J.; Piao, Y.; Yu, B.; Shen, Y.; Zhou, Z. Tuning the Brightness and Photostability of Organic Dots for Multivalent Targeted Cancer Imaging and Surgery. *ACS Nano* **2020**, *14* (5), 5887–5900.

(9) Talanov, V. S.; Regino, C. A. S.; Kobayashi, H.; Bernardo, M.; Choyke, P. L.; Brechbiel, M. W. Dendrimer-Based Nanoprobe for Dual Modality Magnetic Resonance and Fluorescence Imaging. *Nano Lett.* **2006**, *6* (7), 1459–1463.

(10) Kim, Y.; Kim, S. H.; Tanyeri, M.; Katzenellenbogen, J. A.; Schroeder, C. M. Dendrimer Probes for Enhanced Photostability and Localization in Fluorescence Imaging. *Biophys. J.* **2013**, *104* (7), 1566–1575.

(11) Shcharbin, D.; Bryszewska, M.; Mignani, S.; Shi, X.; Majoral, J. Phosphorus Dendrimers as Powerful Nanoplatforms for Drug Delivery , as Fl Uorescent Probes and for Liposome Interaction Studies : A Concise Overview. *Eur. J. Med. Chem.* **2020**, *208*, 112788.

(12) Payne, C. K. Fluorescent Dendritic Nanoprobes: A New Class of Fluorescent Probes for Biological Applications. *Biophys. J.* **2013**, *104* (7), 1394.

(13) Alcala M.A.; Shade C.M.; Uh H., Kwan S.Y.; Bischof M.; Thompson Z.P.; Gogick K. A.; Meier A. R; Strein T. G.; Bartlett D. L; Modzelewski R. A.; Lee Y. J.; Petoud S.; Brown C. K.; Preferential accumulation within tumors and in vivo imaging by functionalized luminescent dendrimer lanthanide complexes. *Biomaterials* **2011**, *32 (35)*, 9343.

(14) Alcala M.A.; Kwan S.Y.; Shade C.M.; Lang M.; Uh H.; Wang M.; Weber S.G.; Bartlett D. L.; Petoud S.; Lee Y. J.; Luminescence targeting and imaging using a nanoscale generation 3 dendrimer in an in vivo colorectal metastatic rat model. Nanomedicine: Nanotechnology, Biology and Medicine **2011**, *7* (3), 249.

(15) Caminade, A.-M.; Hameau, A.; Majoral, J.-P. Multicharged and/or Water-Soluble Fluorescent Dendrimers: Properties and Uses. *Chem. - A Eur. J.* **2009**, *15* (37), 9270–9285.

(16) Choi, S.; Tripathi, A.; Singh, D. Smart Nanomaterials for Biomedics. *J. Biomed. Nanotechnol.* **2014**, *10* (10), 3162–3188.

(17) Almutairi, A.; Guillaudeu, S. J.; Berezin M. Y.; Achilefu S.; Frechet J. M. J. Biodegradable pH-Sensing Dendritic Nanoprobes for Near-Infrared Fluorescence Lifetime and Intensity Imaging. J. Am. Chem. Soc. **2008**,130, 444.

(18) Qiu, J.; Hameau, A.; Shi, X.; Mignani, S.; Majoral, J.-P.; Caminade, A.-M. Fluorescent Phosphorus Dendrimers: Towards Material and Biological Applications. *Chempluschem* **2019**, *84* (8), 1070–1080.

(19) Leclaire, J.; Dagiral, R.; Fery-forgues, S.; Coppel, Y.; Donnadieu, B.; Caminade, A.; Majoral, J.; Cedex, T.; Cnrs, I.; Sabatier, P.; Narbonne, D.; Cedex, T. Octasubstituted Metal-Free Phthalocyanine as Core of Phosphorus Dendrimers : A Probe for the Properties of the Internal Structure. *J. Am. Chem. Soc.* **2005**, *45* (127), 15762–15770.

(20) Soršak, E.; Valh, J. V.; Urek, S. K.; Lobnik, A. Application of PAMAM Dendrimers in Optical Sensing. *Analyst.* **2015**, *140* (4), 976–989.

(21) Koley, S.; Ghosh, S. Encapsulation and Residency of a Hydrophobic Dye within the Water-Filled Interior of a PAMAM Dendrimer Molecule. *J. Phys. Chem. B* **2017**, *8* (121), 1930–1940.

(22) Staneva, D.; Grabchev, I.; Yotova, L.; Betcheva, R. New Glucose Oxidase - Pamam Conjugate as Fluorescent Biosensor Matrix in Acetylcellulose Membrane. *J. Univ. Chem. Technol. Metall.* **2013**, *48* (3), 228–233.

(23) Koley, S.; S. Ghosh. The Study of Electron Transfer Reactions in a Dendrimeric Assembly: Proper Utilization of Dendrimer Fluorescence. *Phys. Chem. Chem. Phys.* **2016**, *18* (36), 24830–24834.

(24) Roberts, J. C.; Bhalgat, M. K.; Zera, R. T. Preliminary Biological Evaluation of Poly(amidoamine) (PAMAM) Starburst™ Dendrimers. *J. Biomed. Mater. Res.* **1996**, *30* (1), 53–65.

(25) Malik, N.; Wiwattanapatapee, R.; Klopsch, R.; Lorenz, K.; Frey, H.; Weener, J. W.; Meijer, E. W.; Paulus, W.; Duncan, R. Dendrimers: Relationship between Structure and Biocompatibility in Vitro, and Preliminary Studies on the Biodistribution of 125I-Labelled Poly(amidoamine) Dendrimers in Vivo. *J. Control. Release* **2000**, *65* (1–2), 133–148.

(26) Li, G.; Shen, L.; Luo, Y.; S. Zhang. The Effect of Silver-PAMAM Dendrimer Nanocomposites on the Performance of PVDF Membranes. *Desalination* **2014**, *338* (1), 115–120.

(27) Cai, Y.; Ji, C.; S. Zhang; Su, Z.; Yin, M. Synthesis of Water-Soluble Dye-Cored Poly(Amidoamine) Dendrimers for Long-Term Live Cell Imaging. *Sci. China Mater.* **2018**, *61* (11), 1475–1483.

(28) Ghosh, S.; Banthia, A. . Towards Fluorescence Sensing Poly(amidoamine) (PAMAM) Dendritic Architectures. *Tetrahedron Lett.* **2002**, *43* (36), 6457–6459.

(29) Georgiev, N. I.; Sakr, A. R.; Bojinov, V. B. Design and Synthesis of Novel Fluorescence Sensing Perylene Diimides Based on Photoinduced Electron Transfer. *Dye. Pigment.* **2011**, *91* (3), 332–339.

(30) Wu, L. P.; Ficker, M.; Mejlsøe, S. L.; Hall, A.; Paolucci, V.; Christensen, J. B.; Trohopoulos, P. N.; Moghimi, S. M. Poly-(Amidoamine) Dendrimers with a Precisely Core Positioned Sulforhodamine B Molecule for Comparative Biological Tracing and Profiling. *J. Control. Release* **2017**, *246*, 88–97.

(31) Wu, L. P.; Ficker, M.; Christensen, J. B.; D. Simberg, D.; Trohopoulos P. N.; Moghimi, S. M. Dendrimer end-terminal motif-dependent evasion of human complement and complement activation through IgM hitchhiking. *Nature Communications*, **2021**, 12, 4858-4871.

(32) Zhang, Q.; Sha, Y.; Wang, J.-H. 8-Hydroxyquinoline Dansylates Modified with PAMAM Dendrimer as Fluorescent Fe3+ Sensors. *Molecules* **2010**, *15* (5), 2962–2971.

(33) Zhao, Y.; Liu, S.; Jiang, W.; Chang, Y.; Li, Y.; Fang, X.; J. Wang. Synthesis and Photoluminescence Study of Di-Dendron Dendrimers Derived from Mono-Boc-Protected Ethylenediamine Cores. *Luminescence* **2011**, *26* (4), 264–270.

(34) Tsai, H.-C.; Imae, T.; Calderõ, G.; Solans, C. Two-Photon Confocal Imaging Study: Cell Uptake of Two Photon Dyes-Labeled PAMAM Dendrons in HeLa Cells. *J. Biomed. Mater. Res. - Part A* **2012**, *100 A* (3), 746–756.

(35) El-Betany, A. M. M.; Vachova, L.; Bezzu, C. G.; Pope, S. J. A.; McKeown, N. B. The Synthesis and Study of Fluorescent PAMAM-Based Dendritic Molecules. *Tetrahedron* **2013**, *69* (39), 8439–8445.

(36) Allen, N. S.; Bentley, P.; Mckellar, J. F. Fluorescence and Light Fastness of Aminoanthraquinones. *J. Photochem.* **1976**, *5*, 225–231.

(37) Allen, N. S.; Mckellar, J. F. Structural Influences on the Fluorescence of Aminoanthraquinones. *J. Photochem.* **1977**, *7*, 107–111.

(38) Inoue, H.; Hida, M.; N. Nakashima; Yoshihara, K. Picosecond Fluorescence Lifetimes of Anthraquinone Derivatives. Radiationless Deactivation via Intra- and Intermolecular Hydrogen Bonds. *J. Phys. Chem* **1982**, *86*, 3184–3188.

(39) Hamanoue, K.; Nakayama, T.; Kajiwara, Y.; Yamaguchi, T.; Teranishi, H. The Lowest Triplet States of Anthraquinone and Chloroanthraquinones: The 1-chloro, 2-chloro, 1,5-dichloro, and 1,8-dichloro Compounds. *J. Chem. Phys.* **1987**, *86*, 6654–6659.

(40) Siddlingeshwar, B.; Hanagodimath, S. M. Estimation of the Ground and the First Excited Singlet-State Dipole Moments of 1,4-Disubstituted Anthraquinone Dyes by the Solvatochromic Method. *Spectrochim. Acta Part A.* **2010**, *75*, 1203–1210.

(41) Zakerhamidi, M. S.; Ghanadzadeh, A.; Moghadam, M. Intramolecular and Intermolecular Hydrogen-Bonding Effects on the Dipole Moments and Photophysical Properties of Some Anthraquinone Dyes. *Spectrochim. Acta Part A.* **2011**, *79*, 74–81.

(42) Choudhari, A. S.; Patil, S. R.; Sekar, N. Solvatochromism, Halochromism, and Azo–Hydrazone Tautomerism in Novel V-Shaped Azo-Azine Colorants – Consolidated Experimental and Computational Approach. *Color Technol.* **2016**, *132*, 387–398.

(43) Perpète, E. A.; Wathelet, V.; Preat, J.; Lambert, C.; Jacquemin, D. Toward a Theoretical Quantitative Estimation of the λmaxof Anthraquinones-Based Dyes. *J. Chem. Theory Comput.* **2006**, (2), 434–440.

(44) Tomalia, D. A.; Baker, H.; Dewald, J.; Hall, M.; Kallos, G.; Martin, S.; Roeck, J.; Ryder, J.; Smith, P. A New Class of Polymers: Starburst-Dendritic Macromolecules. *Polym. J.* **1985**, *17* (1), 117–132.

(45) Krapcho, P. A.; Getahun, Z.; Avery, K. J. The Synthesis of 1,4-Difluoro-5,8-Dihydroxyanthracene-9,10-Dione and Ipso Substitutions of the Fluorides by Diamines Leading to 1,4-Bis-[(Aminoalkyl)Amino]-5,8-Dihydroxyanthracene-9, 10-Diones. *Synth. Commun.* **1990**, *20* (14), 2139–2146.

(46) Navas Diaz, A. Absorption and Emission Spectroscopy and Photochemistry of 1,10-Anthraquinone Derivatives: A Review. *J. Photochem. Photobiol. A Chem.* **1990**, *53* (2), 141–167.

(47) Srivatsavoy, V. J. P.; Venkataraman, B.; Periasamy, N. The Non-Radiative Processes from the S1 State of Aminoanthraquinones: A Steady State and Time-Resolved Study. *J. Photochem. Photobiol. A Chem.* **1992**, *68* (2), 169–184.

(48) Collet, G.; Hrvat, A.; Eliseeva, S. V.; Besnard, C.; Kovalenko, A.; Petoud, S. A Near-Infrared Emitting MOF: Controlled Encapsulation of a Fluorescein Sensitizer at the Time of Crystal Growth. *Chem. Commun.* **2021**, *57* (27), 3351–3354.